Ab initio Fermi surface and conduction-band calculations in oxygen-reduced MoO_3

C. A. Rozzi and F. Manghi
INFM–National Research Center on "nanoStructures and bioSystems at Surfaces" (S^3) and Dipartimento di Fisica, Università di Modena e Reggio Emilia, Modena, Italy

F. Parmigiani
Dipartimento di Matematica e Fisica, Università Cattolica del Sacro Cuore, Brescia, and INFM-TASC, Trieste, Italy
(Received 23 January 2003; published 12 August 2003)

This article reports *ab initio* Fermi surfaces and conduction-band calculations of both stoichiometric and oxygen-reduced MoO_3. The data, based on a TB-LMTO approach in LDA, provide a convincing and detailed interpretation of the one-electron removal XPS valence bands, where a clear energy gap is observed for the stoichiometric samples, whereas a significant emission at the Fermi edge is measured for the oxygen reduced system. In addition, the electrical conductivity, as deduced from the shape of the calculated Fermi surface, is confined in the *xz* plane of the crystal, as required for Luttinger-liquid behavior. These results, when compared to the conduction mechanism observed in the blue bronze $K_{0.3}MoO_3$, clearly suggest that oxygen reduction and doping can bring to very different processes for the electronic transport.

DOI: 10.1103/PhysRevB.68.075106 PACS number(s): 71.18.+y, 71.20.−b, 79.60.−i

I. INTRODUCTION

The understanding of the mechanisms underlying the physical properties of transition metals compounds is currently one of the most compelling problems. In particular, the interplay between the physical properties and the details of the crystal geometry, electronic structure, and stoichiometry is quite obscure. For instance, confining ourselves to the electrical properties, we can find normal metals such as ReO_3 and TiO, large band gap insulators (V_2O_5, Cr_2O_3, α-Fe_2O_3), semiconductors (Cu_2O), compounds that can be subjected to a semiconductor-metal transition (VO_2, V_2O_3, Fe_3O_4, Ti_2O_3), and superconductors ($La_{2-x}Ba_xCuO_4$, $YBa_2Cu_3O_7$).[1]

A particular class of compounds includes V_2O_5, MoO_3, and the compounds obtained by doping these oxides with an alkaline metal. These are effective low-dimensional systems, with a strongly anisotropic conductivity. Focusing on the Mo compounds, it is observed that, while the quasi-1D metallic molybdenum purple bronze ($K_{0.15}MoO_3$) is superconducting, the blue bronze (the $K_{0.3}$ doped oxide) becomes insulator at low temperature, due to the formation of charge density waves,[2] and that the pairing of localized electrons seems to occur without leading to superconductivity. These properties have been subject to intense study,[3–6] and their full comprehension has not been achieved yet.

Among others, the property of the blue bronze to show a Luttinger-liquid physics is still under examination.[4,7] However, the source of its metal character is quite clear: in the blue bronze, potassium behaves similar to a donor of electrons, towards one of the many inequivalent Mo sites. K doping adds both electrons, and new band states to the system, and potassium originating electrons are captured by the lowest energy free orbital of molybdenum. This simple mechanism is accepted to qualitatively explain the conductive behavior of the blue bronze.[8]

As far as the insulating oxide MoO_3 is concerned, we experimentally observe that features similar to those observed in the blue bronze are produced in the gap of the XPS valence band by oxygen reduction. However, the problem of the conductivity in the reduced compound has never been addressed.

This is a very interesting and paradigmatic case where the Fermi surface and the details of the conducting bands can be calculated *ab initio* because of the quite reduced U_{dd} correlation energy, compared to the band width. The aim of this article is to describe the *ab initio* Fermi surface of stoichiometric and reduced MoO_3 and to give a very clear physical background of the electronic structure in these compounds. The calculations, based on a TB-LMTO approach in LDA, also provide atom and orbital resolved DOS that describe the character of the bonds and the transport band properties. Both this information, i.e., Fermi surface and transport properties, provide a map for electrical conduction and band mapping measurements.

We find that the oxygen reduction, though it is not able to add new electrons and new bands to the system, can shift molybdenum $4d$ states into the gap of MoO_3. In addition, the calculations allow one to predict that the conductivity of the reduced compound is strongly anisotropic, mainly occurring in the *xz* plane, unlike that of the blue bronze. This fact is also stressed by the shape of the calculated Fermi surface which does not cross the k_y axis, but intersects k_x and k_z in a few nested sheets.

II. STRUCTURE

MoO_3 has orthorhombic crystal symmetry (see Fig. 1), with lattice parameters $a=3.92$ Å, $b=13.94$ Å, $c=3.66$ Å, and space group *Pbnm*.[9]

The unit cell is made of four MoO_3 units (see Fig. 1). The three oxygen atoms are all inequivalent, and they are grouped into three classes. O′ is coordinated to a single Mo atom at a distance of 1.84 Å, while O″ and O‴ lie approximately in the *xz* plane. Mo-O″ distance is 1.86 Å in two

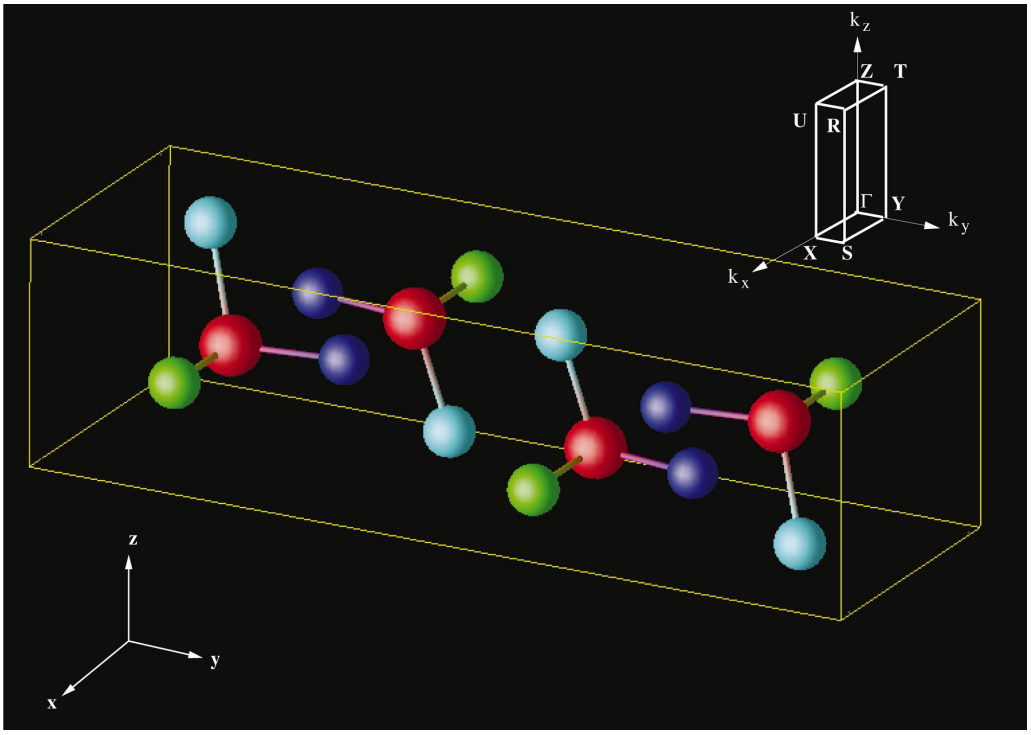

FIG. 1. (Color) The unit cell of orthorhombic MoO_3 has three inequivalent oxygen atoms. Red is Mo, blue O′, green O″, and cyan O‴. Inset: First Brillouin zone with high symmetry lines.

molecules of the cell and 2.05 Å in the others; the Mo-O‴ distance is fixed at 1.90 Å.

For convenience, the bulk can be thought as made of MoO_6 octahedra asymmetrically sharing an O″ atom at a corner. These octahedra are organized in bilayers along the *y* direction. However, these geometrical building units are quite distorted, as they include variable Mo-O bond lengths.[10]

III. STOICHIOMETRIC MoO_3

As a first step we have performed a tight binding LMTO-ASA calculation of the electronic structure of the stoichiometric oxide within the LDA.[11,12] The calculated DOS has an occupied region about 6.7 eV wide, and a small 0.5 eV gap. While we expect that the gap width is underestimated in the LDA, we find good agreement between the calculated and observed valence band width (see Fig. 2).

The atom and orbital resolution (Figs. 3 and 4) of the total DOS (Fig. 2) indicates that the valence band is composed of hybridized O 2*p* and Mo 4*d* states. However, the dominant contribution to the occupied region comes from the O 2*p* band. The Mo 4*d* contribution is quite uniformly distributed in the occupied region, with the exception of the z^2 peak at -6 eV, strongly hybridized with the p_y and p_z components of O‴. Above the Fermi energy, it is possible to recognize (see Fig. 3) that the lowest energy unoccupied levels of Mo have *xy*, *yz*, and *xz* character, while the remaining *d* orbitals raise above 4 eV. The gap has a mixed O-Mo and O-O type, but the dominant character is O-Mo. This fact puts the compound in the class of weakly interacting charge transfer ox-

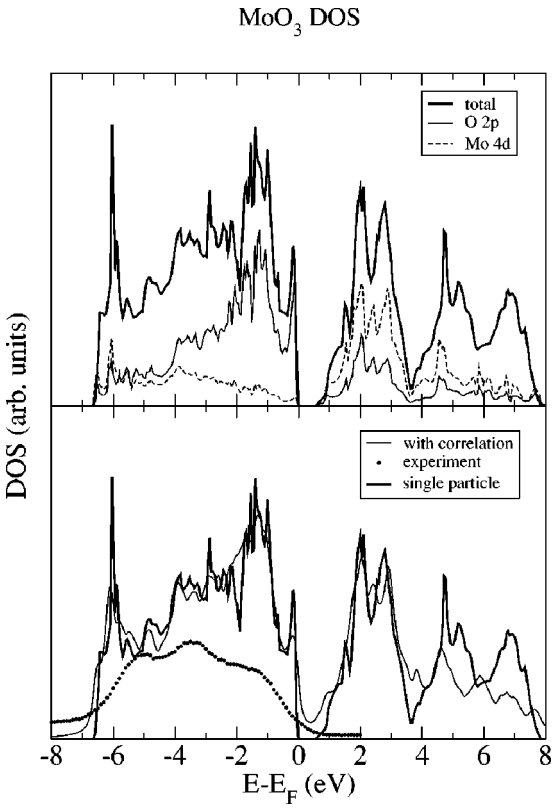

FIG. 2. Upper panel: the calculated LMTO DOS resolved in the main orbital components of each atom type. Lower panel: the solid thick line is the total LMTO-ASA calculated DOS, the dotted line is the spectral function with self-energy correction, convolved with a Gaussian of width 0.5 eV, and dots are XPS experimental points.

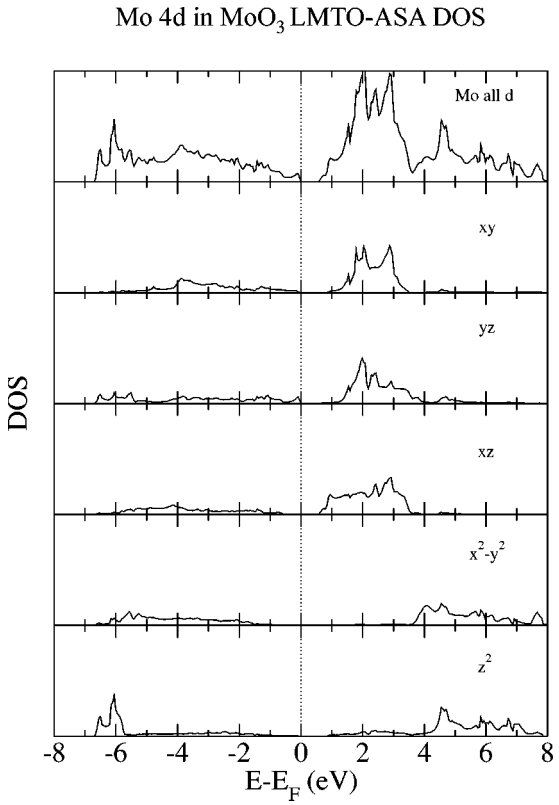

FIG. 3. Calculated orbital Mo 4*d* component of the total LMTO-ASA DOS.

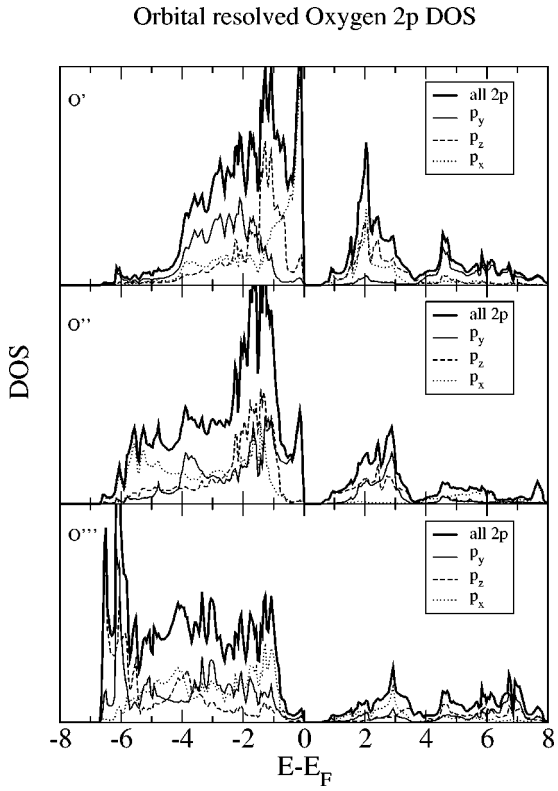

FIG. 4. Orbital and atom resolved oxygen contribution to the total DOS.

ides: we expect a small Coulomb U_{dd} interaction parameter, compared to the valence band width and the insulating gap, and, eventually, to the charge transfer Δ between O and Mo.[13]

The oxygen projected orbital resolution of the DOS (see Fig. 4) also shows that the three oxygen atoms contribute in quite distinct zones of the spectrum to the DOS. In particular, the contribution to the region higher in energy, close to the top band edge, mainly comes from the p_x orbital of O′. The other O atoms contribute to the intensity in the deeper region. The band width of O′ is fairly smaller than that of O″ and O‴. As a matter of fact, its contribution to the total oxygen DOS falls to about zero below -4 eV. This fact indicates a more ionic type of bond than that of the other two oxygen classes. In contrast, both O″ and O‴ have a full 6 eV bandwidth, though their main contributions are, respectively, at -1 and -6 eV, suggesting a covalent bond. This mixed covalent-ionic character is also confirmed by cluster calculations performed for the *xz* surface.[14]

IV. ELECTRON CORRELATION

In addition to the band calculation we have performed a three body scattering (3BS) calculation of the self-energy effects, in order to investigate the role of electron correlation in the one-electron removal XPS valence band. The many body analysis of the photoemission spectrum indicates that no considerable correlation effects are expected in this case, thus enforcing the conclusions obtained within the LDA approach.

The 3BS technique consists of a solid state configuration interaction in which, together with the basic state with a photohole added to the ground state, excited states of the system are allowed to take part to the photoemission process.[15,16] These states are obtained by removing an electron from the occupied valence band, and promoting it to the unoccupied part of the valence band. The total effect on the single particle DOS is a combined effect of the scattering amplitude in the Mo 4*d* band and the value of U_{dd}. This value is treated as a fitting parameter, and it is set to 2 eV for the system under examination.

The results (see Fig. 2) confirm that no such effects are important in the present case, even if a small reduction of the Mo z^2 peak is observed. This fact was expected on the base of the atom resolved DOS analysis, since O-Mo character of the gap suggests that the smallest electron excitation of the system should be an optical one, involving the creation of an oxygen hole and a molybdenum electron. We conclude that the inclusion of correlation effects is not necessary to interpret the XPS valence band of the oxide. Now, let us turn to the examination of the effects of the oxygen reduction.

V. OXYGEN REDUCTION OF MoO_3

The XPS measurements have been performed using a monochromatized Al-$K\alpha$ lamp and a hemispherical analyzer. The pass energy for the analyzer was set at 5 eV. With this parameter the overall energy resolution for the spectrometer was 0.4 eV as measured on the Ag $3d_{5/2}$ core level. The MoO_3 samples were high quality monocrystals cleaved at

10^{-10} mbar. The background pressure during the whole experiment was never higher than 5×10^{-10} mbar. The oxygen reduced MoO_3 was obtained *in situ* by a 1 min mild sputtering of the samples using a 500 eV low current Ar^+ ion flux.

The preferential oxygen sputtering in oxide systems is a well-known mechanism. The O 1*s* and the Mo 3*d* emission lines were used to monitor the reduction effects on the samples. In stoichiometric MoO_3 the Mo 3*d* core lines are symmetric, whereas the O 1*s* line shows a broadening toward the higher binding energy.[17] This broadening, very likely, reflects the different binding energies of the three nonequivalent oxygen ions in the crystal. Unfortunately, the energy resolution in this experiment, i.e., about 0.4 eV, was not sufficient to properly decompose the O 1*s* spectrum and identify the nonequivalent oxygen. Nevertheless, even a very limited oxygen reduction induced a significant splitting of the Mo 3*d* core lines. Therefore, the Ar^+ reduction process was monitored by measuring the intensity of the Mo $3d_{5/2}$ core levels and calculating the ratio between the intensities of the Mo 6+ component versus the Mo reduced components. The sputtering was stopped when the ratio was about 1/1. Also the relative intensity of the O 1*s* emission versus the total Mo 3*d* emission indicates an oxygen reduction of the compounds, however, because of the limited resolution it would be quite ambiguous to infer, from the O 1*s* spectra, about possible preferential sputtering among the nonequivalent oxygen ions in the lattice. Nevertheless the core line photoemission data clearly show that the rise of the gap emission is directly correlated to the enhancement of the oxygen-reduced component in the Mo 3*d* core line spectra. A more prolonged sputtering led eventually to a complete reduction of the Mo ions with a significant enhancement of the emission in the energy gap.

VI. REDUCED MoO_3 VALENCE BAND

The most striking difference between the XPS line shape in the oxygen reduced oxide and in the stoichiometric oxide is the appearance of a feature at the Fermi level, separated by the MoO_3-like band by a deep pin (see Fig. 5).

In order to describe the oxygen reduced oxide we have calculated the DOS in three limiting cases, obtained by creating oxygen vacancies (one oxygen type at a time) and freezing all the remaining atoms to their bulk equilibrium positions. The resulting systems have the same stoichiometry as MoO_2, but they still have the space group symmetry of MoO_3. In the LMTO-ASA approach this is obtained by replacing an oxygen atom with an empty sphere of the same radius. In this way we are able to obtain three DOS's, that describe the reduction process assuming that it amounts to creating oxygen vacancies without destroying the bulk order.

Obviously, this theoretical description of the oxygen-reduced samples is based on rather crude approximations that render the present calculations as model-like. In fact, the oxygen reduction by Ar^+ sputtering is expected to introduce a disordered oxygen reduction rather than an ordered reduction as assumed in the model. Nevertheless, the model helps to rationalize the direct correlation between the oxygen reduction and the emission detected in the energy gap of the one-electron removal valence band spectrum.

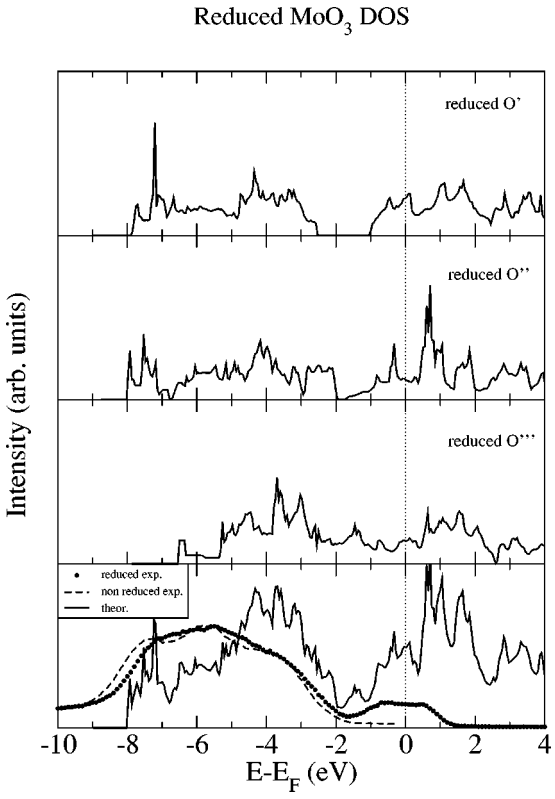

FIG. 5. Single oxygen atom removed from MoO_3 LMTO DOS, and mixing (lowest panel), compared to the experimental XPS. Filled circles refer to the reduced oxides, the dashed line to the stoichiometric MoO_3, as in Fig. 2

A closer look at Fig. 5 clearly shows that, in each one of the three limiting cases, the removal of a single inequivalent oxygen atom has the effect of filling up Mo 4*d* antibonding orbitals located in the gap of stoichiometric MoO_3 while the O 2*p* bonding orbitals still remain occupied, and shift about 2 eV lower in energy, in agreement with the experimental observation. The filled orbitals bond to oxygen along the direction of the longest Mo-O bond distance available. The theoretical one-electron removal XPS valence band can be easily fitted to the experimental one by mixing the three limiting cases. This procedure does not change the qualitative picture of our model, since in every case Mo 4*d* states in the gap appear, but it is performed in order to take into account the fact that oxygen resolution of the reduction process is not available. This method does not account for the effect of disorder, which would require a drastically different approach from the beginning. Finally, in the comparison of the experimental data and the calculated spectra some approximation must be assumed about the cross section of the photoemission process and the normalization of the calculated spectra versus the measured emission. However, the comparison between the experiment and the calculated spectra clearly indicates on a qualitative base the origin of the emission observed in the band gap of oxygen reduced MoO_3.

We conclude that, though the features in the XPS valence band are the same observed in the blue bronze, a different mechanism is to be invoked in order to describe the conduc-

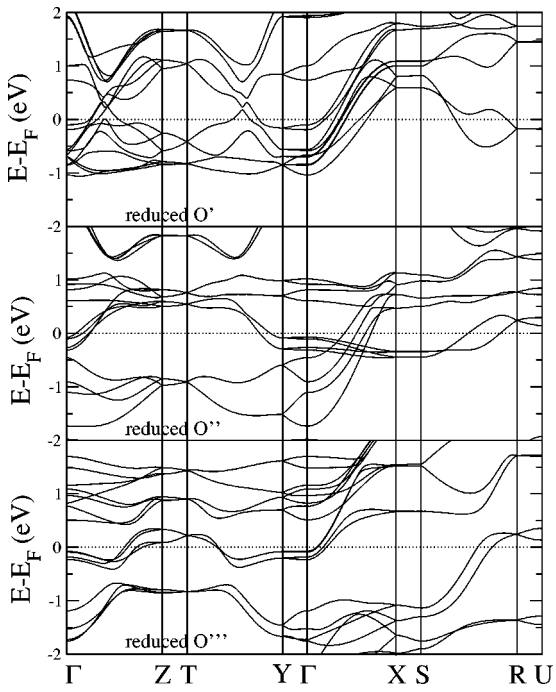

FIG. 6. Single oxygen atom reduced MoO_3 bands around the Fermi energy.

tivity. In fact, the injection of electrons into the system, obtained by K doping, also adds entirely new bands at the Fermi level, while the reduction process creates extended defects, that result in an electron transfer towards the lowest energy free orbitals. These cannot be bondinglike, since the bonding orbitals are already filled, but they are the T_{2g} symmetry Mo 4*d* orbitals, which are the unoccupied lowest energy orbitals.

Finally the band calculation shows (Fig. 6) that, in every case, the bands go across the Fermi level only along the k_x and k_z directions (Γ-X, and Γ-Z, T-Y, S-R in the reciprocal space), while the compound still has an insulating character along the k_y axis (Z-T, Y-Γ, X-S, R-U).

The Fermi surface can be plotted in the three reduced cases (Fig. 7). It is evident the almost equivalent role played by O″ and O‴ atoms lying in the *xz* plane. Removing each of these atoms results in approximately the same Fermi surface shape rotated by 90°. These surfaces show a considerable nesting. Also it can be noted that none of the surfaces cuts the k_y axis, suggesting that no conduction is possible along the *y* direction in the reduced compound.

VII. CONCLUSIONS

In summary, the band analysis, performed in the limiting cases, where a single type of oxygen is removed at a time, shows that the conduction band of the oxygen reduced compound has Mo 4*d* character. We have compared the XPS valence band in the reduced MoO_3 to that of the K doped blue bronze. In spite of the fact that the two line shapes are strikingly similar, we find that a different physical process is the reason of the conductivity properties in these compounds. In fact, while in the case of the blue bronze new Mo 4*d* levels are filled by the electrons added to the system, in the

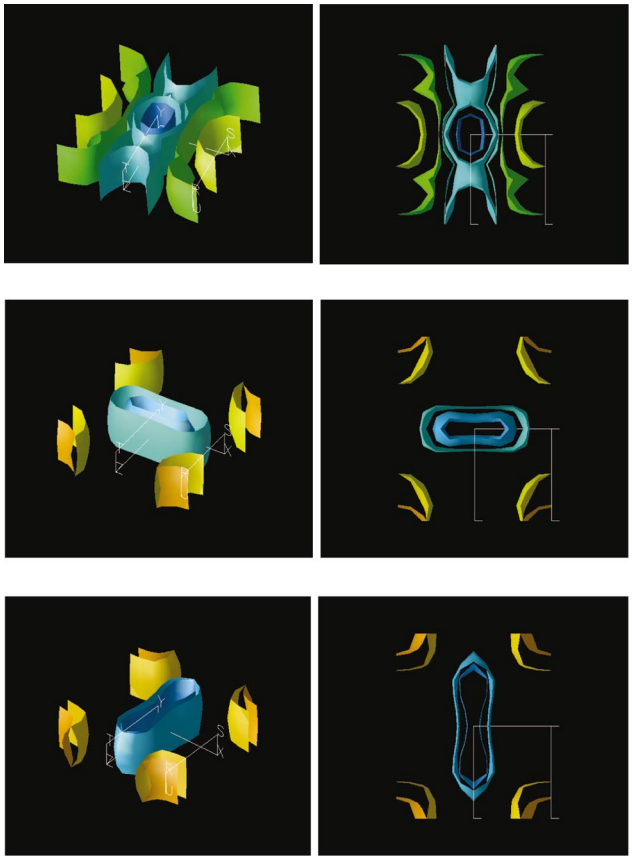

FIG. 7. (Color) Fermi surfaces of the reduced compounds. The upper panel is O′ reduced, the middle is O″ reduced, and the lower is O‴ reduced. The figures on the left are 3D view of the surface in the reduced zone scheme. On the right a top vision of the same surface (i.e., viewing along the k_z axis). The colors are arbitrary, and denote the different band each sheet of the surface originates from.

oxygen reduced MoO_3, these levels are pulled into the gap of MoO_3 by the action of the created extended defects. The differences are also stressed by the plot of the Fermi surfaces, that suggest a two-dimensional conduction for the reduced oxide, while a one-dimensional character for the blue bronze. These findings lead to the conclusion, relevant for the low-dimensional transition metal oxides, that reduction and doping can bring to very different conductive behaviors, though the XPS analysis of the valence band shows very similar features.

In conclusion this paper reports *ab initio* Fermi surfaces of MoO_3 and oxygen reduced MoO_3. From the detailed shape of the calculated Fermi surface, these compounds should exhibit a 2D character in agreement with possible Luttinger-liquid behavior. Finally, the agreement between the calculated density of states, based on a TB-LMTO approach in LDA, provide a convincing interpretation of the one-electron removal XPS valence bands in these systems and constitute the route map for detailed Fermi surface measurements and transport measurements.

ACKNOWLEDGMENTS

C.A. Rozzi thanks Dr. Catia Arcangeli for helpful discussions and friendly collaboration.

[1] *Electronic Conduction in Oxides*, edited by N. Tsuda, K. Siratori, K. Nasu, and A. Fujimori (Springer-Verlag, Berlin, 1991).
[2] *Physics and Chemistry of Low-Dimensional Inorganic Conductors*, edited by C. Schlenker, J. Dumas, M. Greenblatt, and S. van Smaalen, Vol. 354 of *NATO ASI Series B: Physics* (Plenum, New York, 1996).
[3] E. Sandre, P. Foury-Leylekian, S. Ravy, and J.-P. Pouget, Phys. Rev. Lett. **86**, 5100 (2001).
[4] M. Sing, R. Neudert, H. von Lips, M. S. Golden, M. Knupfer, J. Fink, R. Claessen, J. Mücke, H. Schmitt, S. Hüfner, B. Lommel, W. Aßmus, Ch. Jung, and C. Hellwig, Phys. Rev. B **60**, 8559 (1999).
[5] J. L. Mozos, P. Ordejón, and E. Canadell, Phys. Rev. B **65**, 233105 (2002).
[6] J. Demsar, K. Biljaković, and D. Mihailovic, Phys. Rev. Lett. **83**, 800 (1999).
[7] R. Claessen, F. Reinert, G.-H. Gweon, W. P. Ellis, Z. X. Shen, C. G. Olson, L. F. Schneemeyer, F. Lévy, and J. W. Allen, J. Electron Spectrosc. Relat. Phenom. **76**, 121 (1995).
[8] G. K. Wertheim, L. F. Schneemeyer, and D. N. E. Buchanan, Phys. Rev. B **32**, 3568 (1985).
[9] R .W. G. Wyckoff, *Crystal Structures* (Wiley, New York, 1963).
[10] L. Kihlborg, Ark. Kemi **21**, 357 (1963).
[11] O. K. Andersen, Phys. Rev. B **12**, 3060 (1975).
[12] O. K. Andersen and O. Jepsen, Phys. Rev. Lett. **53**, 2571 (1984).
[13] J. Zaanen, G. A. Sawatzky, and J. W. Allen, Phys. Rev. Lett. **55**, 418 (1985).
[14] R. Tokarz-Sobieraj, K. Hermann, M. Witko, A. Blume, G. Mestl, and R. Schlögl, Surf. Sci. **489**, 107 (2001).
[15] F. Manghi, C. Calandra, and S. Ossicini, Phys. Rev. Lett. **73**, 3129 (1994).
[16] S. Monastra, F. Manghi, and C. Ambrosch-Draxl, Phys. Rev. B **64**, 020507 (2001), and references therein.
[17] F. Parmigiani (unpublished).